Supporting Information

Dynamic Asphaltene-Stearic Acid Competition at the Oil-Water Interface

Bastian Sauerer[†], Mikhail Stukan[†], Jan Buiting[‡], Wael Abdallah[*†], Simon Andersen[*§]

[†]Schlumberger Dhahran Carbonate Research Center, Dhahran Techno Valley – KFUPM, P.O. Box 39011, Dammam / Doha Camp 31942, Saudi Arabia

[‡]Retired, formerly Saudi ARAMCO, Reservoir Characterization Department, Dhahran 31311, Saudi Arabia

[§]Schlumberger DBR Technology Center, 9450 – 17th Avenue, Edmonton, AB T6N 1M9, Canada

*Corresponding Authors: wabdallah@slb.com (W.A.) and asphalteam2@gmail.com (S. A.)

Table of Contents

List of Figures

IFT and surface pressure data

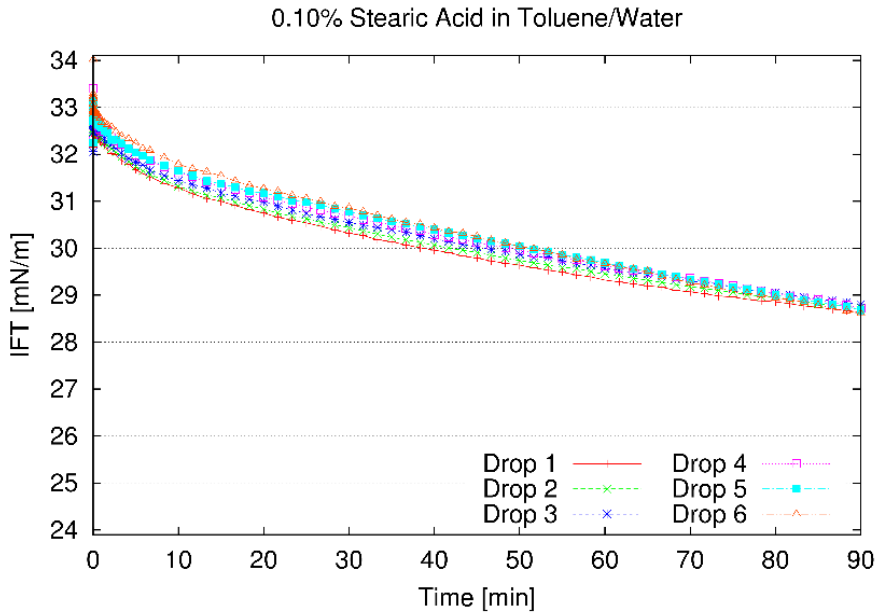

Figure S1. Example of reproducibility of IFT measurements for the case of stearic acid (0.10 wt%).

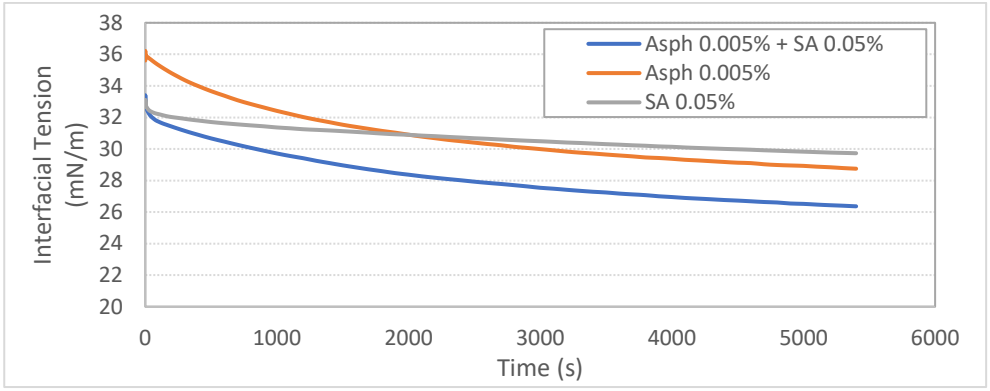

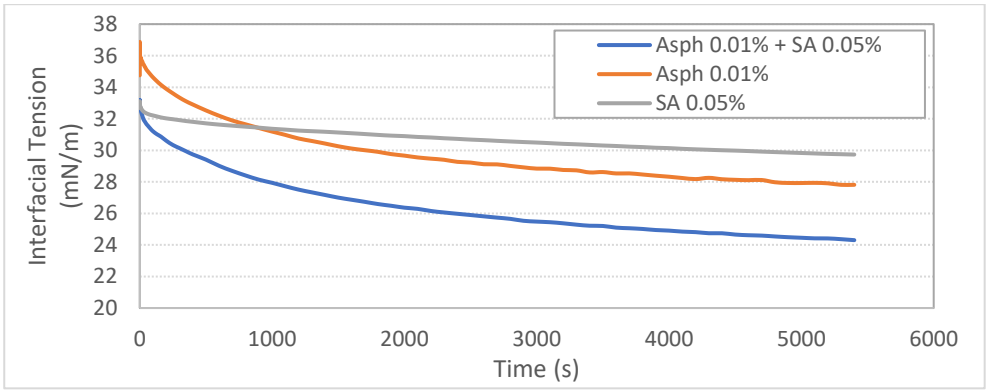

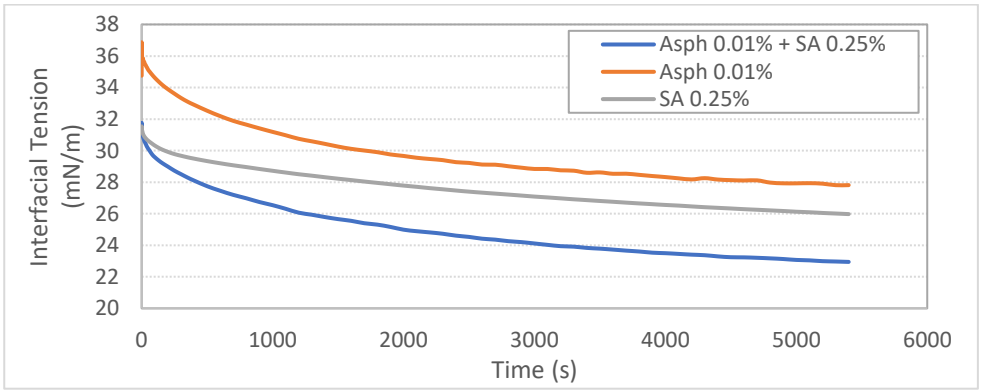

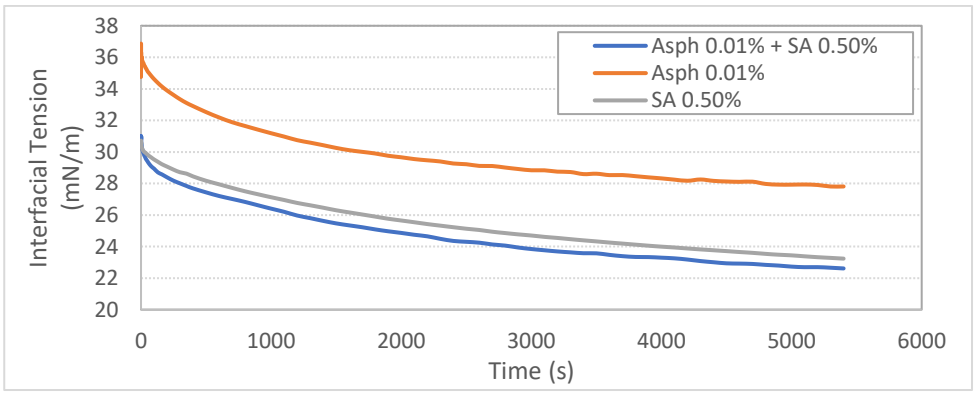

Figure S2. The above 4 figures show the comparison between dynamic interfacial tension of mixtures of asphaltenes and stearic acid and their constituent solutions.

Bulk concentration effects

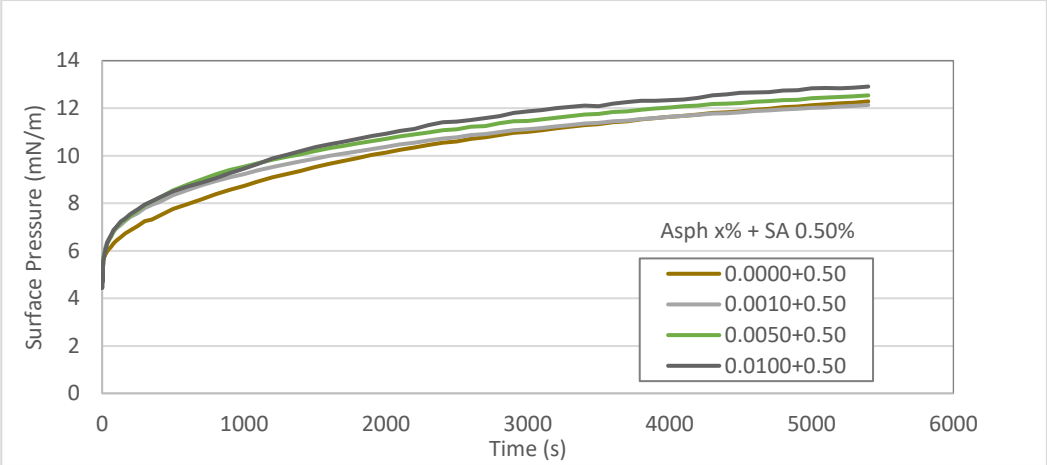

Figure S3. Effect of high bulk concentrations of stearic acid on the asphaltene adsorption. Only small incremental contributions of asphaltenes are observed. This is a direct evidence of the almost complete blocking of the surface by fast adsorbing stearic acid (jump in surface pressure is observed). Concentrations of asphaltenes are between 0.001 wt% and 0.01 wt%.

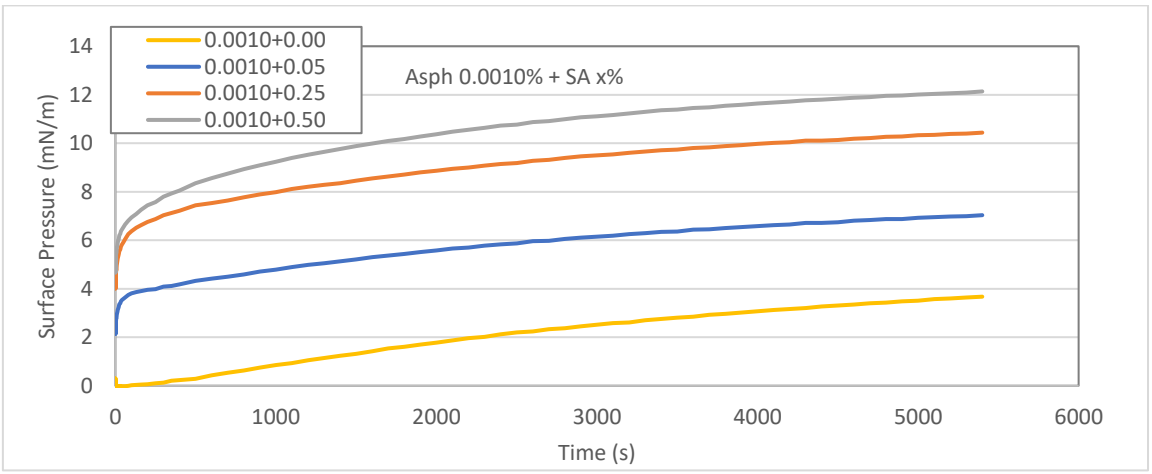

Figure S4. Surface pressures of constant asphaltene concentration (0.001 wt%) solutions with varying stearic acid content. Notice the significant effect of the 0.05 wt% stearic acid.

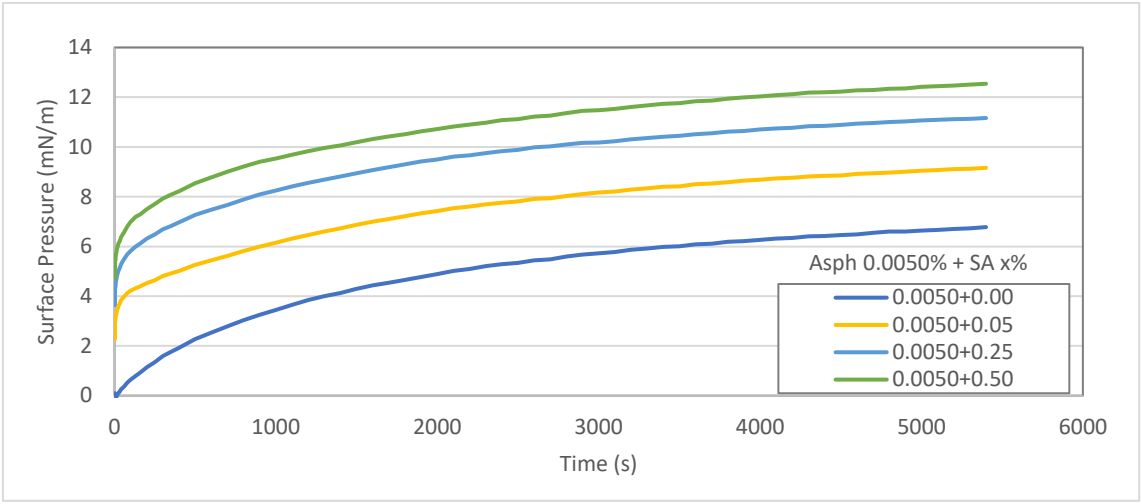

Figure S5. Surface pressures of constant asphaltene concentration (0.005 wt%) solutions with varying stearic acid content.

Pseudo-Equilibrium Data at 5400 sec

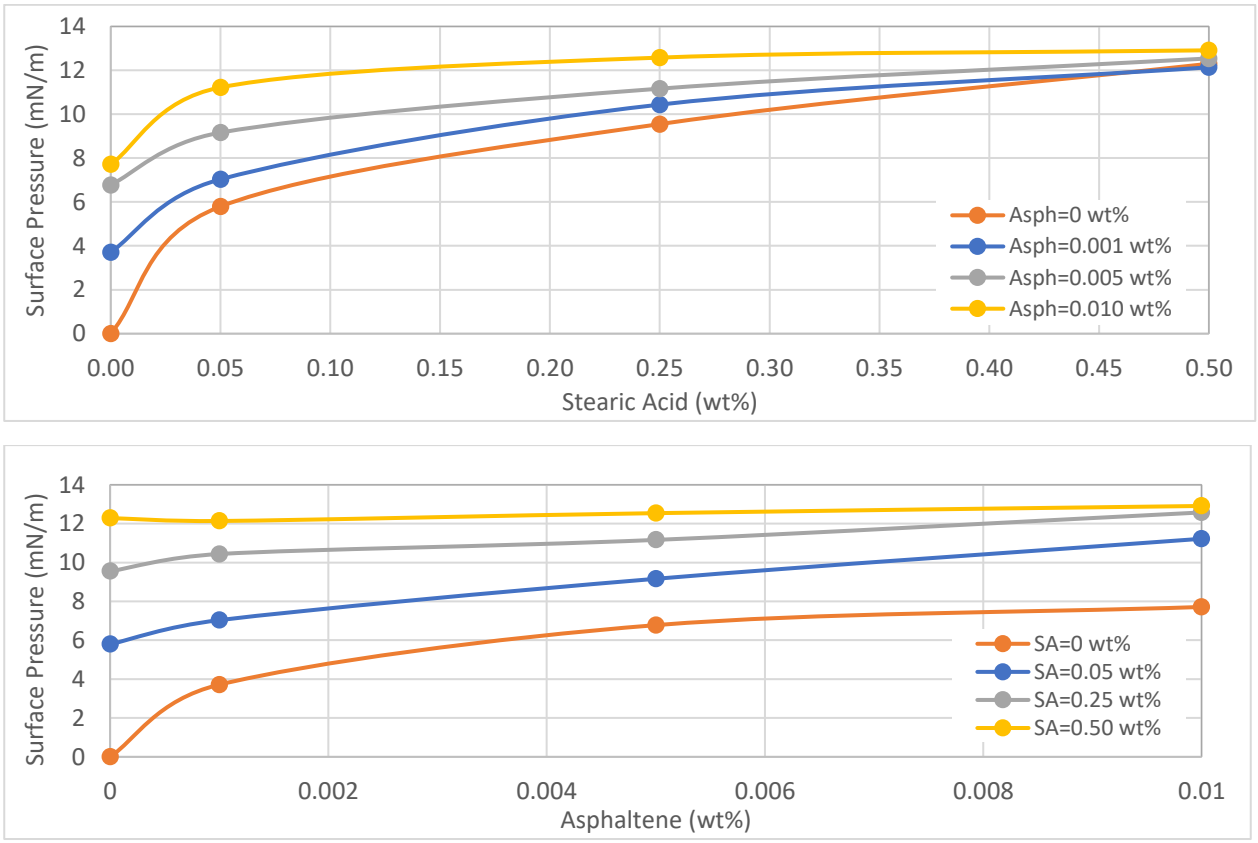

Figure S6. Pseudo-equilibrium surface pressure data at 5400 s for solutions of either asphaltenes or stearic acid and their blends in toluene versus deionized water. The top plot shows stearic acid surface pressure variation at different asphaltene concentration contribution and lower plot shows asphaltene surface pressure variation at different stearic acid concentration contribution.

Surface Pressure Analysis for Binary Asphaltene/Stearic Acid systems

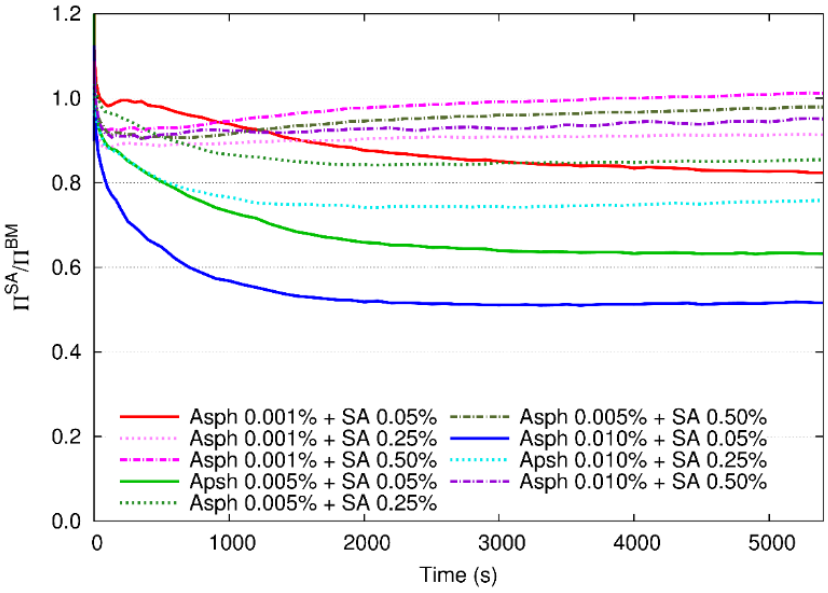

Figure S7. Dynamic surface pressure for water in corresponding stearic acid solutions normalized on surface pressures for water in different binary mixture solutions of asphaltenes (asph) and stearic acid (SA) in toluene.

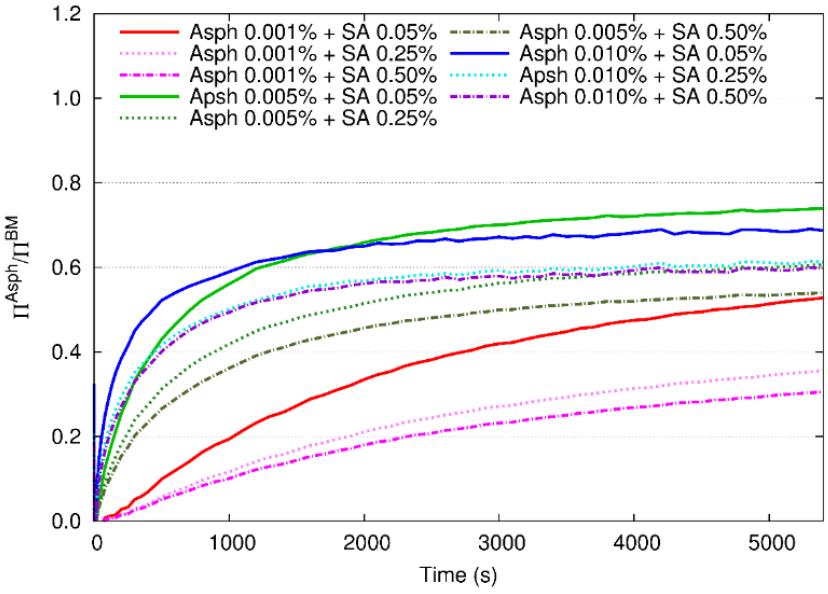

Figure S8. Dynamic surface pressure for water in corresponding asphaltene solutions normalized on surface pressure for water in different binary mixture solutions of asphaltenes (asph) and stearic acid (SA) in toluene.

Note, that the sum of contributions of the individual components in **Figures S7 and S8** is not equal to 1, since the normalization is performed on the binary mixture values, while the impacts of individual components are not additive. Thus, to understand the impact of individual components, one must analyze the leading contribution. In general, it is possible to conclude that asphaltenes come in action only at the late stage of the experiment and in those cases where their concentration is above 0.0050 wt%.

Additional Gibbs-Langmuir Analysis Results

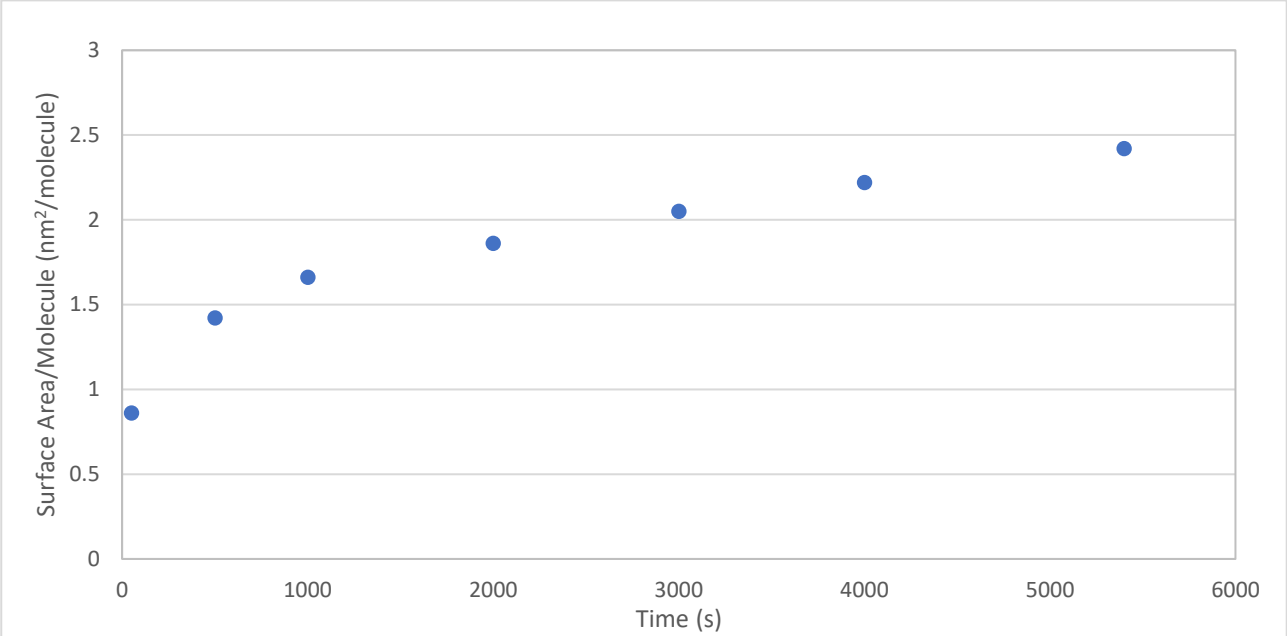

Figure S9. Effect of time on the apparent asphaltene surface area/molecule at the toluene/water interface. With time a steady but larger area is attained indicating the surface is reorganizing (potentially though expelling of certain "fast" but less retained asphaltenes).

Analysis of binary monolayer composition using Rosen's approach

Although there are some indications that the bulk concentration of asphaltenes cannot be used directly in our analysis due to specific adsorption of only a fraction of the species we here attempt a calculation of the monolayer composition based on the approach proposed by Rosen (Rosen, M.J.; Hua, X.Y. Synergism in Binary Mixtures of Surfactants II. Some Experimental Data. J. Am. Oil Chem. Soc. 1982 (59), pp 582-585).

This requires the determination of the concentration (C_i^0) of the individual solutes in the binary mixture that yields the same interfacial tension as the mixture. To estimate this, the Gibbs relation was applied and linear correlations between ln C_i and γ (at pseudo equilibrium) were established for solutions of either SA or asphaltenes. This was used to establish (C_i^0) for both SA and asphaltenes at the interfacial tension of each of the mixtures. Rosen devised the following relation:

$$\frac{(X_1)^2 \ln(C_1 / C_1^0 X_1)}{(1-X_1)\ln\left[C_2 /(C_2^0(1-X_{1)}\right]} = 1 \qquad \text{Equation A1.}$$

Where X_1 is the mole fraction of species 1 in the binary monolayer and C_i and C_i^0 are respectively the molar concentration of the bulk solution and the established concentration at which $\gamma_{mix} = \gamma_i$. The molecular weight of asphaltenes was assumed to be 1000 g/mol.

After establishing the Gibbs correlations and establishing C_i^0 for all mixtures one can solve equation A1 iteratively for X_1.

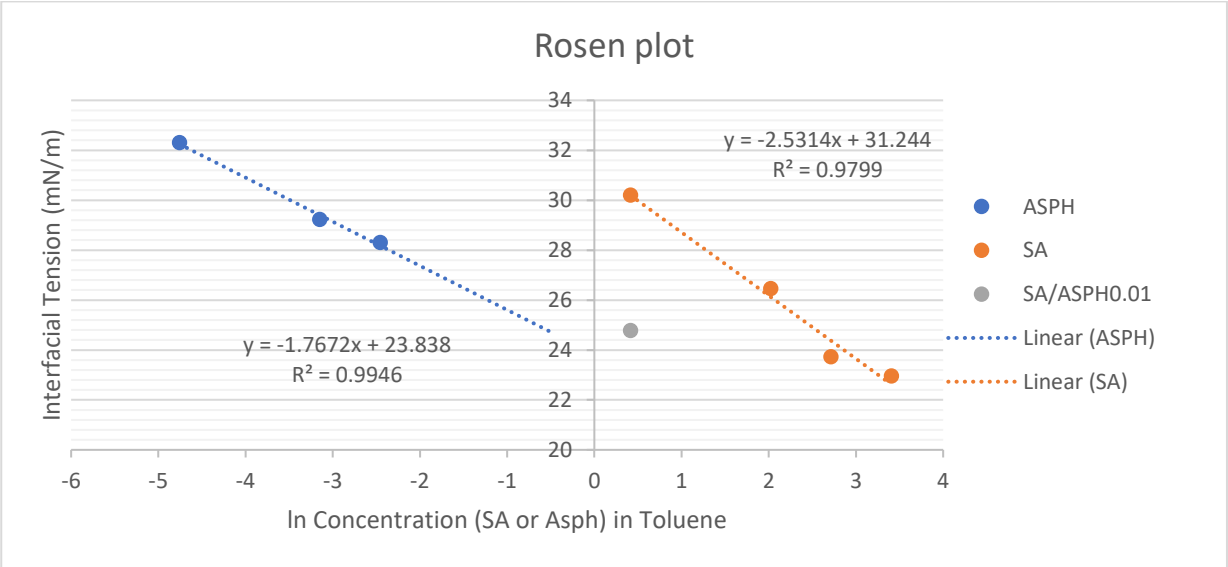

Figure S10. Gibbs correlation for solutions of either SA or asphaltenes with the indication of the solution of the mixture 0.05 wt% SA and 0.01 wt% asphaltenes.

Additional Diffusion Analysis by Ward-Tordai approach

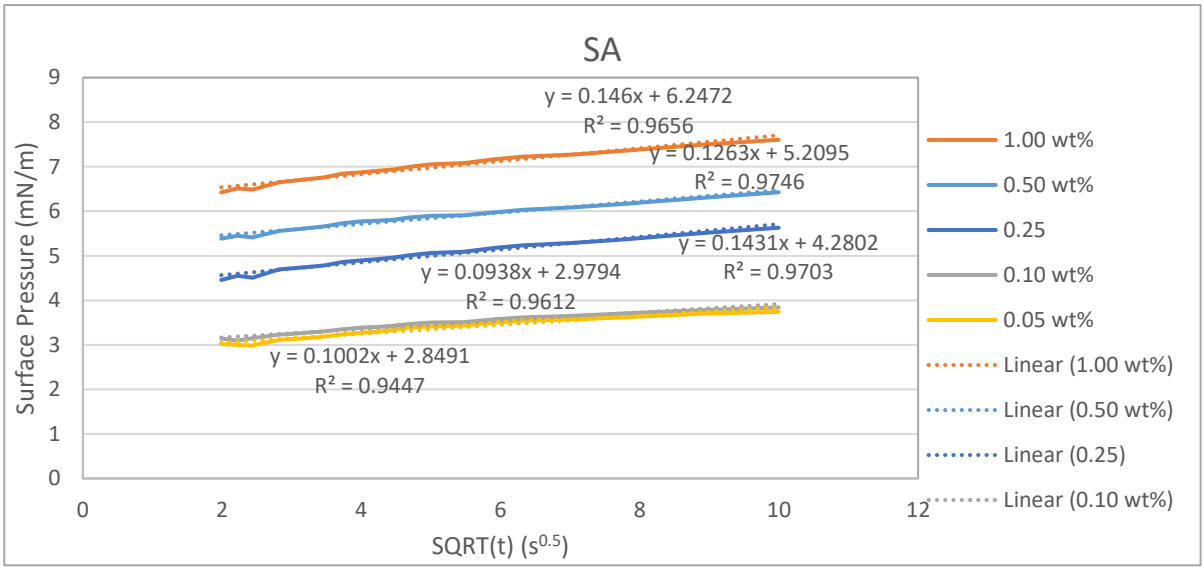

Figure S11. Diffusion analysis of the long term surface pressure development for stearic acid solutions.

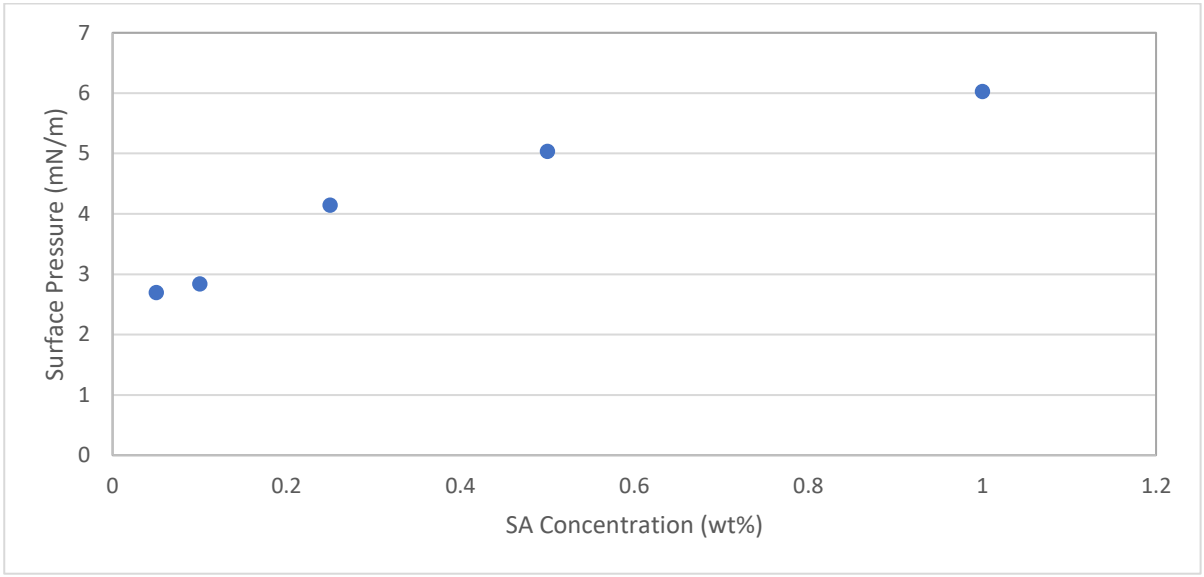

Figure S12. Initial surface pressure from intercept of the diffusion analysis (Intercept PI(t=0) vs. SQRT (t)) versus stearic acid concentration. Notice the regular increase.

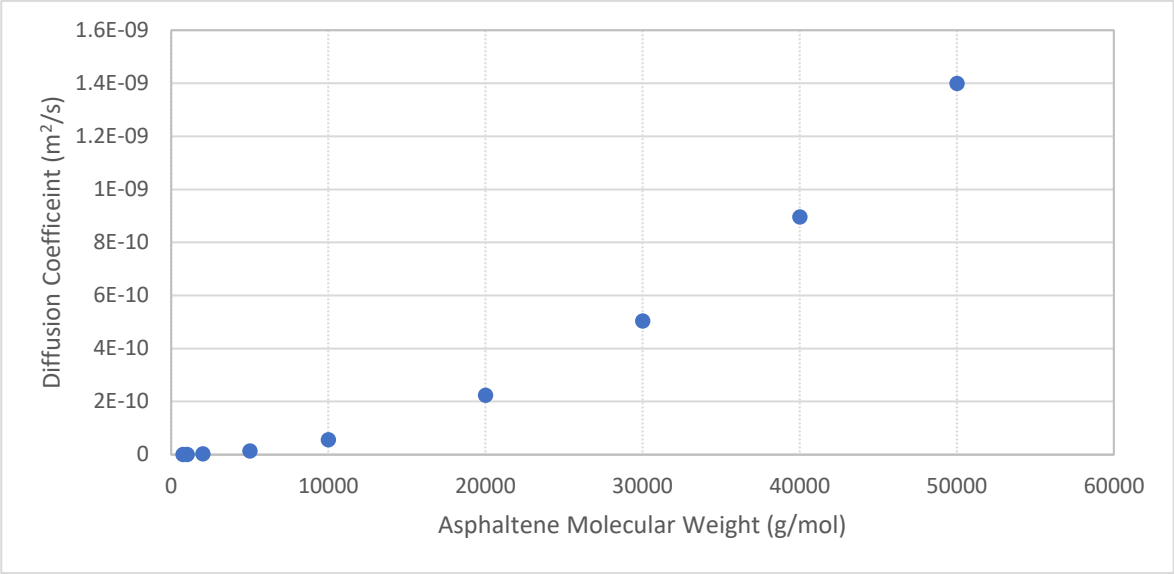

Figure S13. Effect of the estimated molecular weight on the diffusion coefficients for the short term approach. It is observed that the effect of molecular weight fairly shallow at the normal range of asphaltene MWs below 5000 g/mol.

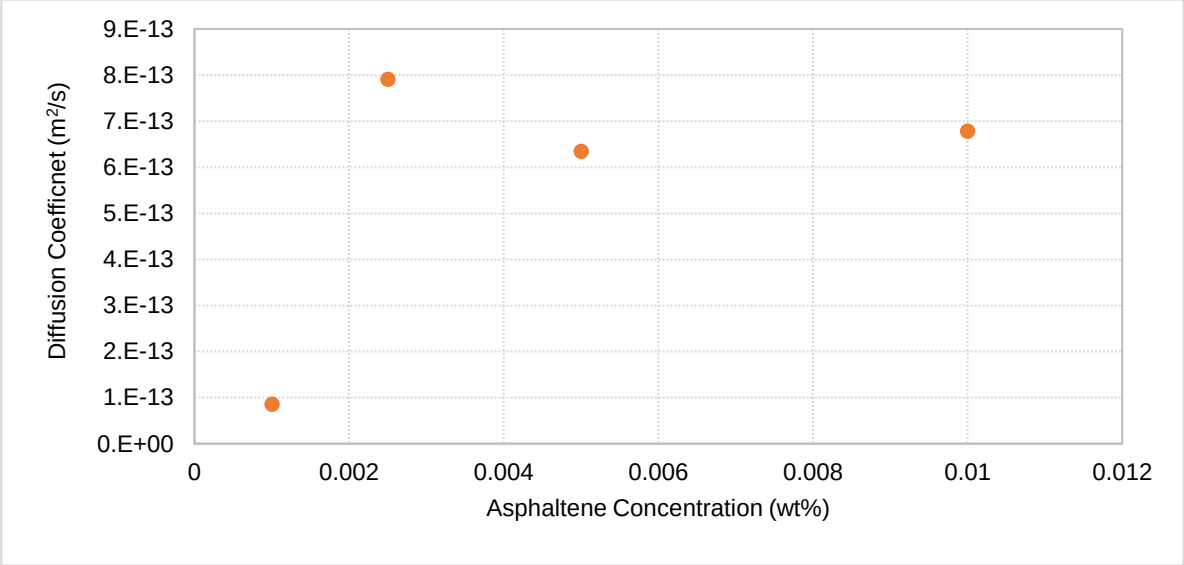

Figure S14. Diffusion coefficients as a function of asphaltene concentration derived from the short term model. Notice the significant jump at low concentrations which is opposite of the one observed for the long term approach.

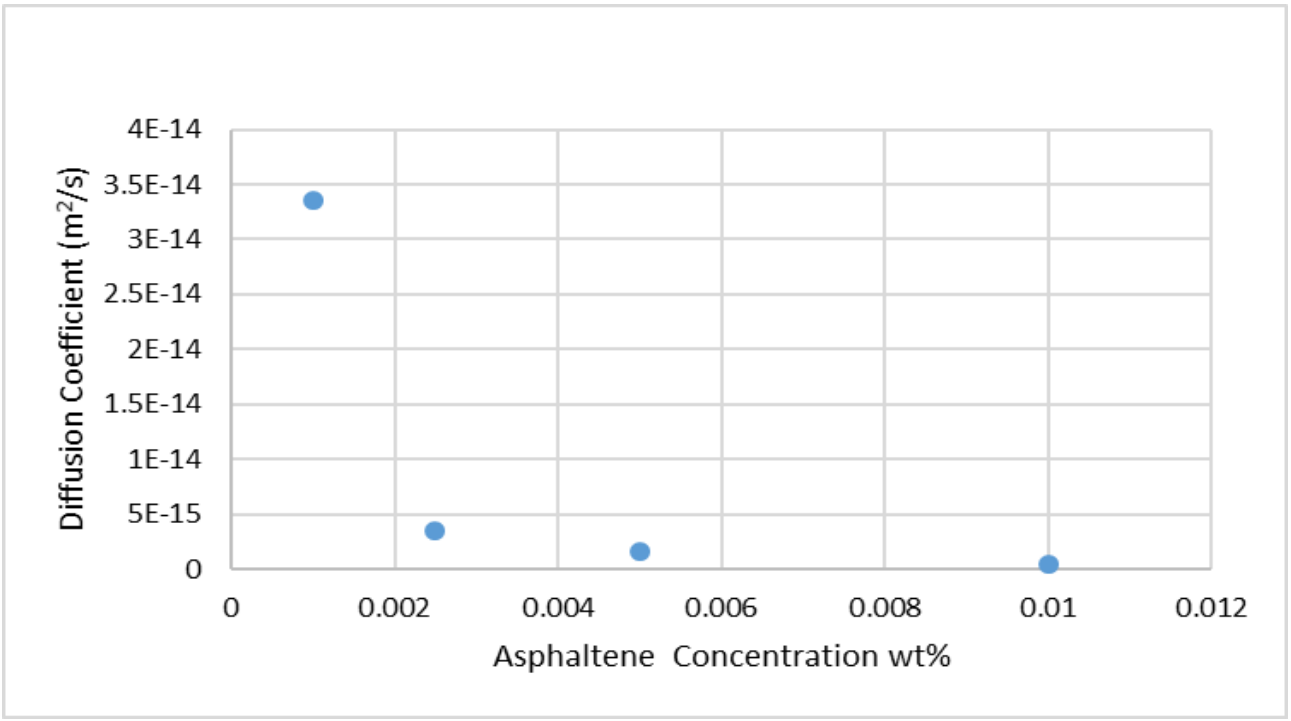

Figure S15. Diffusion coefficients at long term diffusion (>3000 seconds) as a function of asphaltene concentration.